Petroleum Science 23 (2026) 1636–1649

Contents lists available at ScienceDirect

Petroleum Science

journal homepage: www.keaipublishing.com/en/journals/petroleum-science

Original Paper

Carbon isotopes of asphaltene-occluded hydrocarbons: A proxy for bitumen vein source identification in northwest Sichuan Basin, China

Peng Fang [a,b,*], Jia Wu [b,c,**], Xue-Min Xu [a], Bin Shen [a], Wei-Lin Sun [a], Xiao Jin [d], Feng Chen [e], Ning-Ning Zhong [b], Ming-Hui Zhou [f]

[a] National Research Center for Geoanalysis, Beijing, 100037, China
[b] College of Geoscience, China University of Petroleum (Beijing), Beijing, 102249, China
[c] State Key Laboratory of Organic Geochemistry, Guangzhou Institute of Geochemistry, Chinese Academy of Sciences, Guangzhou, 510640, Guangdong, China
[d] Key Laboratory of Coupling Process and Effect of Natural Resources Elements, Natural Recourses Survey, CGS (CNRS), Beijing, 100055, China
[e] Institute of Geochemistry, Chinese Academy of Sciences, Guiyang, 550081, Guizhou, China
[f] State Key Laboratory of Enhanced Oil and Gas Recovery, PetroChina Research Institute of Petroleum Exploration and Development, Beijing, 100083, China

ARTICLE INFO

Article history:
Received 10 February 2025
Received in revised form
6 October 2025
Accepted 11 November 2025
Available online 20 November 2025

Edited by Xi Zhang and Jie Hao

Keywords:
Bitumen veins
Asphaltenes
Adsorbed/occluded hydrocarbons
Carbon isotopes
Organic matter source
Sichuan Basin

ABSTRACT

The Lower Cambrian bitumen veins in northwestern Sichuan Basin originated from Precambrian paleo-oil reservoirs, yet the severe alterations of bitumen and high maturity of potential source rocks challenge conventional oil-source correlation. In this study, we focus on analyzing the stability of carbon isotopic compositions in asphaltene-occluded hydrocarbons to reveal their preservation of original organic signatures. Asphaltenes from the solid bitumen were investigated through gold tube closed-system thermal simulation experiments (300–400 °C). Free saturated hydrocarbons in raw samples exhibit ^{13}C-enrichment ($\delta^{13}C = -31.3‰$) due to biodegradation, while thermal simulation experiments reveal progressive ^{13}C-depletion of free saturated hydrocarbons ($\Delta\delta^{13}C = -4.7‰$) caused by kinetic isotope effects during thermal cracking. In contrast, asphaltene-occluded saturated hydrocarbons maintain exceptional $\delta^{13}C$ stability ($-28.5‰ \pm 0.2‰$) across the same stages, demonstrating complete protection by macromolecular shielding, and adsorbed hydrocarbons display intermediate behavior with moderate $\delta^{13}C$ shifts, indicating partial shielding at asphaltene surfaces. Biomarker distributions (C_{27}-dominant steranes, *n*-alkane bimodality, and *n*-alk-(1)-enes) in occluded hydrocarbons probably preserve original signatures unaffected by secondary alterations. The combined $\delta^{13}C$ signature (within the $-26‰$ to $-31‰$ range characteristic of shallow-water Doushantuo Formation) and biomarker evidence (consistent with Precambrian eukaryotic algal contribution) in occluded hydrocarbons conclusively identify the Ediacaran Doushantuo Formation as the bitumen source. These results demonstrate that asphaltene nanoaggregates effectively shield occluded components from secondary alterations and thermal maturation to a certain extent, providing reliable proxies for Precambrian oil-source correlation in altered reservoirs.

1. Introduction

The outcropping of bitumen veins in the northwestern Sichuan Basin of China is thought to be derived from Precambrian paleo-oil reservoir, which is probably the critical evidence of primary oil and gas resources in the Meso-Neoproterozoic (Wang and Han, 2011). Accurately revealing the source of these bitumen veins is significant for understanding the enrichment of organic matter and oil and gas resource potential of Meso-Neoproterozoic strata in Sichuan Basin. However, the formation of bitumen veins through complex tectonic uplift and subsequent secondary alterations,

* Corresponding author.
** Corresponding author.
E-mail addresses: fangpeng@mail.cgs.gov.cn (P. Fang), jia.wu@cup.edu.cn (J. Wu).

Peer review under the responsibility of China University of Petroleum (Beijing).

https://doi.org/10.1016/j.petsci.2025.11.024

including biodegradation, water washing, and oxidation, has substantially modified the original geochemical signatures in the bitumen (Fang et al., 2021). Moreover, the high thermal maturity of regional source rocks (Liang et al., 2009) has caused convergence in conventional biomarker distributions (e.g. steranes and terpanes), rendering standard oil-source correlation methods ineffective. Consequently, correlating the bitumen with the potential source rock represents a significant challenge.

Numerous solid bitumen veins are exposed in the Kuangshanliang area, northwestern Sichuan Basin (Huang and Wang, 2008). Currently, the source of these bitumen veins remains controversial between two candidate formations: Ediacaran Doushantuo and Lower Cambrian Qiongzhusi formations. Wang and Han (2011) explained the main geological origin of the bitumen veins as a consequence of tectonic movements that disrupted paleo-oil reservoirs with a large amount of liquid petroleum. The presence of dolomitic and siliceous inclusions from the Precambrian period in the bitumen veins led to the conclusion that the black shale of the Doushantuo Formation was the source of the bitumen (Han et al., 2022; Wang and Han, 2011). Furthermore, the Re-Os isotope dating of solid bitumen indicated ages between 572 and 559 million years ago (Wang et al., 2016a), thereby supporting the hypothesis that the bitumen originated from the source rocks of the Doushantuo Formation. On the other hand, the analysis of biomarkers (e.g., sterane distributions) in the bitumen and the potential source rocks by catalytic hydropyrolysis indicates that the bitumen was derived from the Qiongzhusi Formation (Fang et al., 2022c). Nevertheless, the composition of the substances released by catalytic hydropyrolysis may not be representative for the original one due to alterations of the biomarker distributions at high temperatures (Fang et al., 2022a). Moreover, the generally low signal-to-noise ratio of compounds in biomarker chromatograms of bitumens or seep oils subjected to catalytic hydropyrolysis (Fang et al., 2022c) also impairs the reliability of biomarker interpretation. As a result, the source of bitumen remains an open question.

Essentially, identifying the comparable original geochemical information in both bitumen and its potential source rock simultaneously is key to resolving the dispute. It has been shown that the carbon isotope values ($\delta^{13}C$) of kerogen undergo minimal change (±0.3‰) during the generation of hydrocarbons in source rocks (Lewan, 1983). Thus, the organic carbon isotope values ($\delta^{13}C_{org}$) of the two potential source rocks (Doushantuo and Qiongzhusi formations) are likely to retain their original characteristics. However, surface oxidation can significantly alter the carbon isotopes of bitumen (Liang et al., 2020), thereby precluding the direct tracing of oil sources from the isotopic composition of bitumen. Encouragingly, it has been found that the macromolecular structures of asphaltenes can trap (adsorb or occlude) some native small molecules, protecting them from biodegradation and thermal alteration (Cheng et al., 2016, 2017; Fang et al., 2022a; Kashirtsev, 2018; Liao et al., 2006b; Snowdon et al., 2016; Zhao et al., 2010). It is hypothesized that the carbon isotopic compositions of asphaltene-occluded hydrocarbons remain stable despite potential oxidation of bulk asphaltenes, as the occluded components are shielded within the core nanoaggregate regions of asphaltene macromolecules. This spatial protection prevents isotopic alteration by secondary processes (e.g., oxidation, biodegradation), allowing occluded hydrocarbons to retain original source signatures. Consequently, these fractions may provide reliable insights into the origins of bitumen veins.

While previous research has demonstrated the utility of occluded hydrocarbons for preserving molecular (biomarker) information (Fang et al., 2022a, 2022b), a critical gap remains in systematically testing the stability of their carbon isotopic signatures under thermal maturation and applying this specific parameter to resolve oil-source correlation. The primary objectives of this study are therefore: (1) to experimentally verify the hypothesis of carbon isotopic stability for asphaltene-occluded hydrocarbons during thermal maturation; (2) to assess the degree of isotopic decoupling between occluded, adsorbed, and free fractions; and (3) to utilize the robust $\delta^{13}C$ signature of the occluded hydrocarbons to conclusively identify the source of the Kuangshanliang bitumen veins, thereby providing a novel solution to this longstanding debate.

To achieve these objectives, we sampled bitumen veins from the Lower Cambrian Changjianggou Formation in the Kuangshanliang area of northwest Sichuan. Free hydrocarbons as well as those adsorbed and occluded by asphaltenes were isolated by conventional separation and dispersive solid-phase extraction (Fang et al., 2022b). The thermal maturation experiments were conducted to investigate the stability and decoupling of carbon isotope values in adsorbed and occluded components. Finally, the bitumen source was deduced by comparing the carbon isotopes of the occluded hydrocarbons with those found in potential source rocks reported by previous studies.

2. Material and methods

2.1. Sample and geological background

The bitumen veins in the Lower Cambrian Changjianggou Formation outcrop are located in the Kuangshanliang area, which is situated in the northwest Sichuan Basin and within the Longmen Mountain Nappe structure belt (Fig. 1) (Wu et al., 2012). It is commonly accepted that the bitumen veins in this region are not directly derived from source rocks, but formed as a consequence of tectonic damage to the Ediacaran paleo-oil reservoir (Huang and Wang, 2008; Wang et al., 2014). Due to the combined effects of biodegradation, washing, and weathering, the bitumen has undergone significant oxidation. Recent studies have shown that the equivalent vitrinite reflectance of bitumen veins is approximately 0.6% and that they contain a substantial quantity of soluble organic matter, with asphaltenes exceeding 80% (Fang et al., 2021; Liang et al., 2020; Wu et al., 2020). In this study, a solid bitumen sample was taken from the Lower Cambrian Changjianggou Formation outcrop (Fig. 1).

2.2. Experiments

2.2.1. Sample pretreatment

Dichloromethane (DCM) was used to extract soluble organic matter from crushed bitumen powder, followed by filtration to remove all mineral residues prior to isotopic analysis. This rigorous pretreatment ensured the complete separation of organic fractions from any carbonate or mineral matrix, thereby eliminating potential contamination that could influence $\delta^{13}C$ measurements. Excess petroleum ether (boiling range 30~60 °C, ≥95% nC_5~nC_6 alkanes), a solvent composition functionally equivalent to *n*-hexane, was used to precipitate asphaltenes from the extract (Wang et al., 2019; Zhu et al., 2022), allowing the separation of free maltenes by filtration. The asphaltene precipitate was purified by centrifugal elution, which yielded the fraction of asphaltene-adsorbed maltenes (Fang et al., 2021; Liao et al., 2006c; Wu et al., 2020). In this procedure the asphaltenes were re-dissolved in a small amount of DCM, re-precipitated with an excess of petroleum ether and centrifuged at 3500 rad/min for 20 min. The procedure was repeated 3–5 times until the supernatant petroleum ether was almost colourless (Zhao et al., 2010). All supernatant petroleum ether fractions were combined and

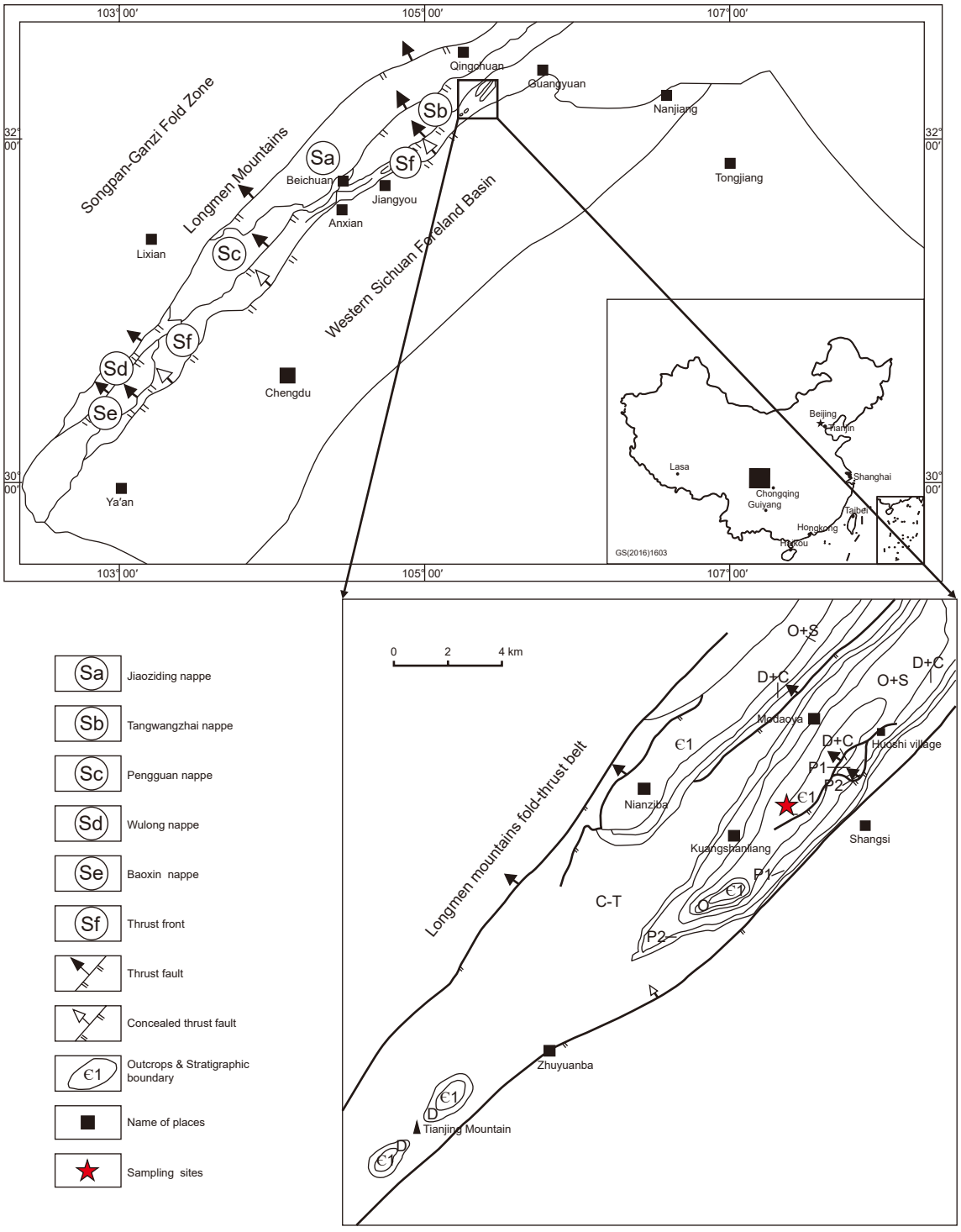

Fig. 1. Tectonic sketch map of the Kuangshanliang area of the Sichuan Basin (modified after Wu et al., 2012).

concentrated to isolate the asphaltene-adsorbed maltenes. At the same time, the purified asphaltenes were collected.

2.2.2. Thermal maturation experiments

Gold-tube experiments were conducted in an ST-120-II apparatus under rigorously controlled conditions (Landais et al., 1989; Michels and Landais, 1994; Monthioux et al., 1985; Wu et al., 2020). The length, the inner diameter, and the wall thickness of the gold tube were 60, 5.5, and 0.25 mm, respectively. Each tube was first heated to approximately 800 °C with a butane-air torch for 3 min to remove all residual organic materials on its wall, then welded on one end using a PUK U4 microscope argonarc welder (Wu et al., 2022). Each gold tube was filled with approximately 30 mg of asphaltenes and 100 mg of deionized water. The other end of gold tube was weld after the sample was loaded. The thermal maturation experiments were held at temperatures of 300, 350 and 400 °C (±1 °C precision) under a constant pressure of 30 MPa (±0.1 MPa precision). The application of confining pressure

in the range of 20–50 MPa is a standard practice in pyrolysis studies to simulate the confined geo-pressure conditions typical of the oil window (Li et al., 2022; Michels and Landais, 1994; Wu et al., 2021). For the purpose of this study, which is to investigate the fundamental behavior and relative stability of different hydrocarbon occurrences (free, asphaltene-adsorbed/occluded) under controlled, geologically realistic conditions, this established experimental parameter is robust and appropriate. All reactors were heated to the target temperature within 1 h, and held at this temperature for 24 h. The corresponding calculated equivalent vitrinite reflectance values (using the Easy%R_o calculation scheme) (Sweeney and Burnham, 1990) for 300, 350 and 400 °C were 0.64%, 0.92% and 1.49%, respectively. These Easy%R_o values simulate maturation stages spanning the early oil window (R_o = 0.6%–1.0%) to the peak oil window (R_o = 1.0%–1.5%).

The solid bitumens in the Kuangshanliang area originated from paleo-reservoir destruction (Wang et al., 2014). Despite the high-over maturity of marine source rocks in the Sichuan Basin Palaeozoic and older strata (Liang et al., 2009), these bitumens were isolated from the source rock thermal regime during reservoir leakage (Wang et al., 2014), preserving a lower thermal maturity (equivalent R_o ~0.6 %) (Liang et al., 2020). In addition, the 300–400 °C range is suitable to simulate hydrocarbon generation from low-maturity bitumen, avoiding unrealistic over cracking (>450 °C), such as aromatic ring cracking (Lorant and Behar, 2002). Therefore, the thermal simulation of the sample with the set maturity range conforms to the general law of its natural evolution, and is also the forward modeling of the possible process in the study area.

2.2.3. Post-treatment of the product

The reactors were allowed to cool down at the end of the experiment, and the gold tubes were removed for subsequent analysis. After opening the gold tubes, the product was extracted with petroleum ether to collect the free maltenes. Then the asphaltenes were extracted with DCM. Subsequently, the asphaltene-adsorbed maltenes were isolated by the above purification treatment (Wu et al., 2020). The occluded hydrocarbons within purified asphaltenes were isolated using a nondestructive dispersive solid-phase extraction (DSPE) method, following an optimized protocol from our prior study (Fang et al., 2022b). The detailed step-by-step DSPE procedure is described in the Supplementary Materials. In brief, the method involves dispersing asphaltene clusters in dilute DCM and utilizing silica gel to physically adsorb polar macromolecules and thus separate the occluded maltenes without chemical alteration (Fig. 2). This method was chosen over oxidative degradation or pyrolysis due to its ability to effectively release occluded hydrocarbons while avoiding the introduction of oxidative damage or thermal cracking effects (Fang et al., 2022b; Snowdon et al., 2016).

The maltenes (both from the raw sample and the post-pyrolysis product) in the three different fractions (free, asphaltene-adsorbed, occluded) were separated into compound groups by liquid–solid chromatography using a silica gel-alumina column. The saturated hydrocarbons were eluted with 30 mL petroleum ether. A mixture (20 mL) of DCM/petroleum ether (volume ratio 2/1) was used to elute the aromatic hydrocarbons. Finally, the polar components (resins) were eluted with 20 mL of a DCM/methanol mixture (volume ratio 9/1) (Zhu et al., 2022). The detailed experimental flow chart is shown in Fig. 3.

2.3. Analysis

2.3.1. Isotopic analysis of organic carbon

The $\delta^{13}C$ analysis of fractions was conducted using a gas chromatography-isotope ratio mass spectrometry (FLASH HT EA-MAT 253 IRMS) system following the Chinese petroleum industry standard SY/T 5238-2019 (Analysis method for carbon and oxygen isotope of organic matter and carbonate), with all values

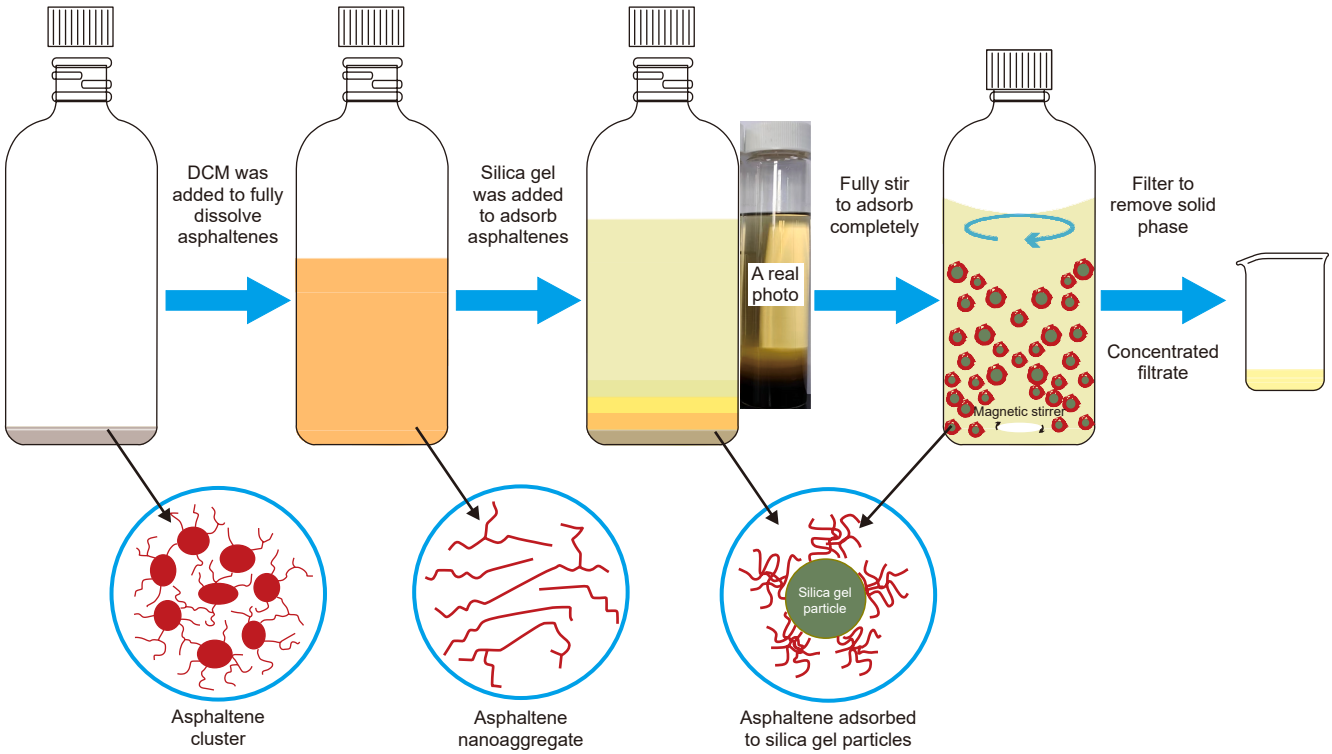

Fig. 2. Schematic diagram of dispersive solid-phase extraction method.

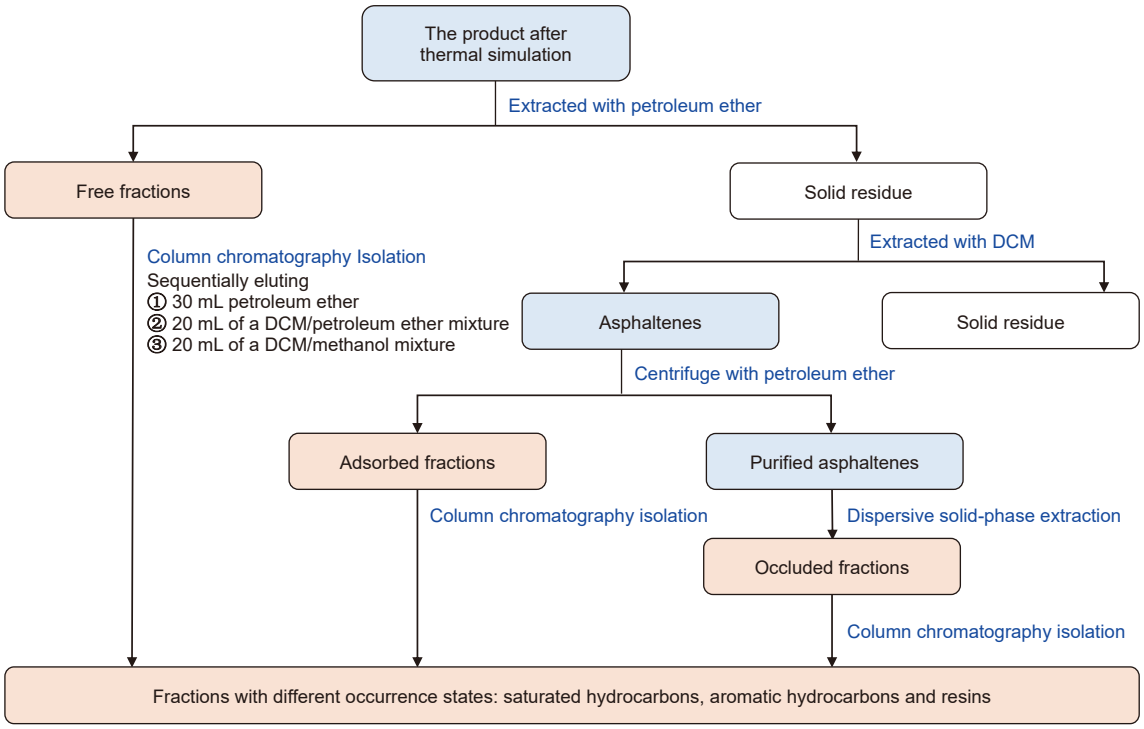

Fig. 3. Flow chart of post-treatment of thermal simulation experiment product.

reported in per mil (‰) relative to the Vienna PDB standard. The analytical conditions were optimized to ensure complete combustion and precise measurement. Helium was used as the carrier gas with a flow rate of 100 mL/min. High purity oxygen with flow rate of 250 mL/min was used as combustion improver. The oxidation reactor was filled with chromium oxide, copper, and silver-containing cobalt oxide and run at a temperature of 980 °C. Standard samples are used for daily calibration of the instrument, including GBW04408 ($\delta^{13}C = -36.9‰$), IAEA-600 Caffeine ($\delta^{13}C = -27.771‰$), USGS62 Caffeine ($\delta^{13}C = -14.79‰$), and USGS24 Graphite ($\delta^{13}C = -16.05‰$). Standard samples were analyzed in parallel with samples to validate accuracy, and laboratory crude oil internal standard ($\delta^{13}C = -27.0‰$) was used for batch-to-batch consistency. Repeated measurements of standards yielded a standard deviation of ±0.2‰, consistent with SY/T 5238-2019 requirements.

Product mass and biomarker data for the samples in aforementioned experiments have been characterized in our previous research (Fang et al., 2022a). The product mass data is determined by an electronic balance with a precision of 0.1 mg, and the distribution of biomarkers (*n*-alkanes, terpanes, and steranes) was based on GC–MS analysis of saturated hydrocarbons. These data, originally published to investigate thermal hysteresis of asphaltene-trapped hydrocarbons, are reused here solely to validate $\delta^{13}C$-based interpretations. Full methodological details and raw data are available in the cited study (Fang et al., 2022a).

3. Results

The $\delta^{13}C$ value of the total DCM-extractable organic matter of the bitumen veins was −35.5‰. After removal of the free hydrocarbons and the asphaltene-adsorbed hydrocarbons, the $\delta^{13}C$ value of asphaltenes was −36.4‰. The carbon isotopic compositions of the three compound groups of the free and asphaltene-adsorbed and the occluded hydrocarbons are listed in Table 1. All fractions are isotopically heavier (enriched in ^{13}C) than the total DCM extract (−35.5‰) and the purified asphaltenes (−36.4‰), with $\delta^{13}C$ values ranging from −35.1‰ to −27.8‰.

In the products of the thermal maturation experiments, the $\delta^{13}C$ values of the free and adsorbed saturated hydrocarbons decreased with temperature. Furthermore, the adsorbed saturated hydrocarbons ($\delta^{13}C$ values: −27.8‰ at 300 °C; −28.5‰ at 350 °C; −29.6‰ at 400 °C) (Table 1) were enriched in ^{13}C as compared to those of the corresponding free saturated hydrocarbons ($\delta^{13}C$ values: −29.5‰ at 300 °C; −32.8‰ at 350 °C; −34.2‰ at 400 °C) (Table 1). The $\delta^{13}C$ values of free/adsorbed aromatic hydrocarbons and resins were generally lower (enriched in ^{12}C) than those of the corresponding saturated hydrocarbons. The $\delta^{13}C$ values of occluded hydrocarbons changed little with temperature. In particular, the $\delta^{13}C$ values of occluded saturated hydrocarbons were stable at −28.7‰ ~ −28.3‰. The $\delta^{13}C$ values of occluded aromatic hydrocarbons and resins were relatively similar, ranging from −32.2‰ ~ −30.8‰.

To contextualize the $\delta^{13}C$ signatures of products, product yields and biomarker distributions from Fang et al. (2022a) were reanalyzed. The quantitative composition data of different components in the experimental products was shown in Table 2. For raw sample, asphaltenes constitute >80% of the soluble organic matter (>30% of bulk bitumen; Table 2) in bitumen, making them the dominant reservoir of source information. The key observations of biomarker distributions include three aspects. (1) Free/adsorbed hydrocarbons: pronounced unresolved complex mixture (UCM) in total ion current chromatogram profiles of raw free hydrocarbons confirms secondary alterations, while a distinct series of *n*-alkanes was detected in raw adsorbed hydrocarbons (Fig. 4); Thermal cracking dominates *n*-alkane and sterane/terpane distributions of free/adsorbed hydrocarbons at 300–400 °C, as evidenced by the progressive shift toward lower carbon-number homologs (Fig. 5). (2) Occluded hydrocarbons: Stable *n*-alkane and sterane/terpane distributions across temperatures (Fig. 5) align with $\delta^{13}C$

Table 1
Carbon isotope values (‰) of the free and asphaltene-adsorbed/occluded fractions.

Fractions	Sate	Raw	300 °C	350 °C	400 °C	Range Min ~ Max	Δ (Max−Min)
Saturates	Free	−31.3	−29.5	−32.8	−34.2	−34.2 ~ −29.5	4.7
	Adsorbed	−28.4	−27.8	−28.6	−29.6	−29.6 ~ −27.8	1.8
	Occluded	−28.7	−28.5	−28.4	−28.3	−28.7 ~ −28.3	0.4
Aromatics	Free	−34.5	−29.8	−33.4	−33.9	−34.5 ~ −29.8	4.7
	Adsorbed	−34.0	−33.2	−33.8	−35.1	−35.1 ~ −33.2	1.9
	Occluded	−31.9	−30.9	−32.2	−30.8	−32.2 ~ −30.8	1.4
Resins	Free	−32.8	−30.5	−32.4	−32.6	−32.8 ~ −30.5	2.3
	Adsorbed	−35.0	−31.7	−35.1	−34.1	−35.1 ~ −21.7	3.4
	Occluded	−31.5	−31.0	−31.7	−31.4	−31.7 ~ −31.0	0.7

Notes: "Raw" refers to the sample that have not been subjected to thermal simulation experiments. The measurement error of carbon isotope value is ±0.2‰. Δ = Maximum value−minimum value across all samples (raw and thermal simulation temperatures of 300~400 °C), representing the total fluctuation range of parameters.

Table 2
Masses and corresponding yields of the free and asphaltene-adsorbed/occluded fractions.

Fractions	Raw		300 °C		350 °C		400 °C	
	Weight, mg	Yield, %	Weight, mg	Yield, %	Weight, mg	Yield, %	Weight, mg	Yield, %
Free saturates	0.9[a]	0.8[a]	0.4[c]	1.3[c]	1.4[c]	4.6[c]	2.9[c]	9.6[c]
Free aromatics	7.4[a]	6.5[a]						
Free resins	9.5[a]	8.4[a]						
Asphaltenes	93.7[a]	82.8[a]	20.3	66.6	15.5	50.7	3.0	9.9
Adsorbed saturates	1.9[a]	1.7[a]	<0.1	<0.3	<0.1	<0.3	<0.1	<0.3
Adsorbed aromatics	1.2[a]	1.1[a]	0.2	0.7	<0.1	<0.3	<0.1	<0.3
Adsorbed resins	4.5[a]	4.0[a]	1.2	3.9	0.9	2.9	1.0	3.3
Purified asphaltenes	83.8[a]	74.0[a]	18.9	62.0	14.6	47.7	2.0	6.6
Occluded saturates	0.5[b]	2.7[b]	0.4	1.3	0.3	1.0	0.2	0.7
Occluded aromatics	0.1[b]	0.5[b]	0.3	1.0	<0.1	<0.3	<0.1	<0.3
Occluded resins	1.3[b]	7.0[b]	0.5	1.6	0.3	1.0	0.3	1.0

Note: "Raw" refers to the sample that have not been subjected to thermal simulation experiments.
[a] Qualities and corresponding yields of products isolated from the original extract (113.2 mg) of solid bitumen (the mass percentage of the original extract in bitumen sample is 35.6%).
[b] Qualities and corresponding yields of occluded components isolated from a certain amount of purified asphaltene (13.7 mg of purified asphaltene obtained from 18.5 mg of extract).
[c] Due to the low absolute mass, the free fractions were not weighed after isolated, so only the qualities and corresponding yields of maltenes before isolated were presented. The yields of raw samples are obtained by dividing the mass of each fraction by the mass of the extract. The yields of thermal simulation experiment products are obtained by dividing the mass of each fraction by the mass of purified asphaltene used in the experiment (30.5 mg at 300 °C; 30.6 mg at 350 °C; 30.3 mg at 400 °C). The original data in the table comes from the reanalysis of our previous study (Fang et al., 2022a).

invariance (−28.5‰ ± 0.2‰), demonstrating asphaltene protection of original signatures. (3) Biomarker parameters: based on the reanalysis of biomarker data, a series of potential biomarker parameters that can be used for oil source correlation are re-counted (Table 3). The variation law of most parameters with temperature is the same as that of $\delta^{13}C$ value, showing the characteristics of stable occluded hydrocarbon parameters and obvious fluctuation of free/adsorbed hydrocarbon parameters (Table 3).

4. Discussion

4.1. Heterogeneous $\delta^{13}C$ distributions of different components from the bitumen

In contrast to isotopic trends for components in crude oil (Stahl, 1978), the $\delta^{13}C$ value of free saturated hydrocarbons separated from the original sample was significantly higher (enriched in ^{13}C) than that of aromatic and polar components (Fig. 6). In general, with increasing polarity, crude oil components are more enriched in ^{13}C, possibly resulting in the $\delta^{13}C$ value of polar components being 3‰–4‰ higher than that of non-polar components (Stahl, 1977). However, different geochemical histories of crude oil may result in heterogeneous isotope distributions (Chung et al., 1981). Biodegradation of non-polar hydrocarbons in crude oil preferentially consumes isotopically lighter species without significantly changing the carbon isotopic composition of the aromatic components (Stahl, 1980). This leads to relative enrichment of ^{13}C in the residual saturated hydrocarbons and relative enrichment of ^{12}C in the resulting aspalthenes in biodegradation-associated bitumen. Previous biomarker analyses of the solid bitumen samples of the study area clearly indicated that the solid bitumen has undergone severe biodegradation (Fang et al., 2021, 2022c; Wang et al., 2014). The pronounced UCM in the free hydrocarbon TIC and the characteristic biomarker patterns (e.g., depleted *n*-alkanes; short-chain sterane dominance) further confirm moderate-to-severe biodegradation in the raw sample (Fig. 4). Therefore, it is probable that biodegradation caused the free saturated hydrocarbons from solid bitumen to be enriched in ^{13}C.

The adsorbed and occluded saturated hydrocarbons that extracted from the raw asphaltene exhibited $\delta^{13}C$ values that were approximately 3‰ higher (enriched in ^{13}C) than those of the free saturated hydrocarbons (Fig. 6). The $\delta^{13}C$ values of the occluded aromatics and resins were found to be >1‰ higher (enriched in ^{13}C) than those of the corresponding free components (Fig. 6). In general, adsorbed or occluded components are protected from biodegradation by the macromolecular structure of asphaltene (Ma et al., 2008; Orea et al., 2021; Pan et al., 2002; Wu et al., 2020). Additionally, they are also relatively stable during thermal evolution and may have a diagenetic origin (Fang et al., 2022a; Galimov, 2006; Meredith et al., 2008; Yang et al., 2009). Conversely, the

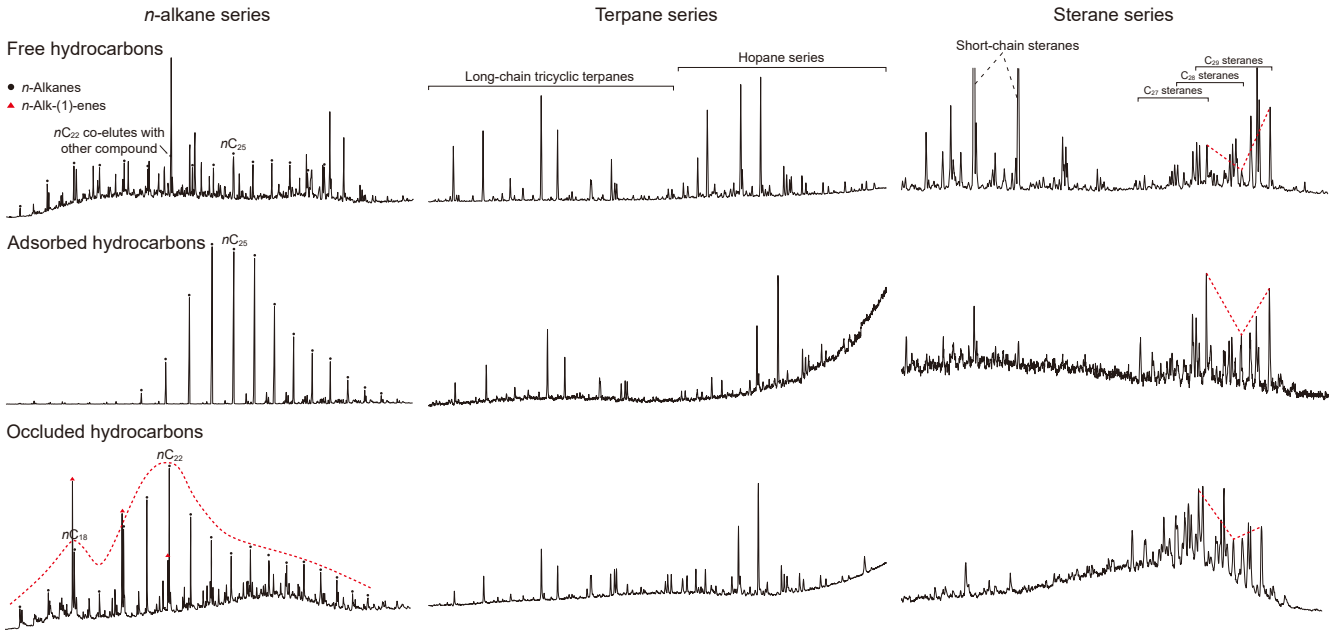

Fig. 4. Distributions of biomarkers in raw bitumen sample (The distributions of *n*-alkanes are based on total ion current chromatograms, TIC; The distributions of terpanes are based on *m/z* 191 selected ion monitoring chromatograms; The distributions of steranes are based on *m/z* 217 selected ion monitoring chromatograms.) The drawing data comes from our previous study (Fang et al., 2022a).

carbon isotopic compositions of free hydrocarbons, i.e., those related to the thermal maturation of organic matter, are also affected by biodegradation. It can thus be concluded that the carbon isotopic composition of asphaltene-occluded hydrocarbons is not a result of biodegradation. Rather, it may be related to the original source of organic matter.

During the diagenetic process, organic matter undergoes complex biogeochemical reactions, leading to the formation of kerogen (Bushnev and Burdel'Naya, 2009). In this process, certain non-thermogenic, original saturated hydrocarbons (biomarkers) derived from organisms become occluded within the macromolecular structure of kerogen. When kerogen undergoes thermal degradation to generate substantial amounts of asphaltene, these occluded saturated hydrocarbons are subsequently inherited into the asphaltene structure (Cheng et al., 2017). Therefore, the asphaltene-occluded saturated hydrocarbons may retain the biogeochemical influences experienced during diagenesis. Nevertheless, since the precursor kerogen also underwent the same biogeochemical processes during its formation, the carbon isotopic compositions of the occluded saturated hydrocarbons and kerogen should theoretically remain comparable. However, the aromatic and polar compounds occluded in asphaltene do not possess direct biological relevance. These components are more likely derived from the thermal degradation of kerogen and subsequently occluded into the macromolecular structure alongside original saturated hydrocarbons in localized regions of the kerogen matrix. This results in the carbon isotopic compositions of the occluded aromatics and polar compounds being influenced by primary thermal cracking, leading to lower $\delta^{13}C$ values (Fig. 6) due to kinetic fractionation effects. It can be inferred that although different hydrocarbon components occluded in asphaltene structure are protected during late-stage thermal evolution, only the occluded saturated hydrocarbons can maximally preserve the original characteristics of the organic matter.

It is expected that differences in $\delta^{13}C$ values between asphaltene-occluded and free hydrocarbons are inevitable for geological samples that have undergone complex geological evolution. In certain specific geological cases, this discrepancy is interpreted as a result of mixing or multi-stage charging of crude oil (Tian et al., 2012a, 2012b; Zhao et al., 2010). For instance, it has been observed that asphaltene-occluded *n*-alkanes in marine crude oil from the Tarim Basin, northwest China, were significantly more enriched in ^{13}C than free *n*-alkanes and it is speculated that this resulted from mixing of crude oil from Middle–Upper Ordovician source rocks and Cambrian-Lower Ordovician source rocks (Tian et al., 2012a, 2012b). In addition, previous researchers observed a similar phenomenon in their study of carbon isotope composition of asphaltene-occluded hydrocarbons in Ordovician ZG31 bitumen from the Tarim Basin and speculated that this was related to multi-stage charging of crude oil (Zhao et al., 2010). While these interpretations remain plausible hypotheses, they lack definitive biomarker evidence to conclusively establish oil mixing or multi-stage charging. More importantly, thermal maturation effect and secondary alterations are likely to result in complicated alterations to the geochemical characteristics of free hydrocarbons. This is often observed in the case of occluded hydrocarbons and free hydrocarbons, which exhibit disparate carbon isotope compositions. Therefore, it is necessary to carefully evaluate the reasons for the enrichment of ^{13}C in asphaltene-occluded hydrocarbons in specific geological cases. At 300 °C, the $\delta^{13}C$ values of saturated hydrocarbons, aromatic hydrocarbons, and resins in different states were found to be higher (enriched in ^{13}C) than the corresponding values in the original sample (Fig. 3). It can be generally observed that pyrolysis at 300 °C does not result in significant cleavage of asphaltene macromolecules, as evidenced by previous studies (Fang et al., 2022a; Jia et al., 2017; Wu et al., 2020; Xiong and Geng, 2000). The asphaltene sample employed in the thermal maturation experiments had been purified, thereby excluding the majority of interference from the original free and adsorbed hydrocarbons. Nevertheless, trace quantities of strongly adsorbed hydrocarbons that might persist on the asphaltene structure could readily diffuse under thermal stress (Wu et al., 2020). Consequently, the isotopic compositions of the newly formed free and adsorbed hydrocarbons that emerge during thermal treatment were different from those of the original components.

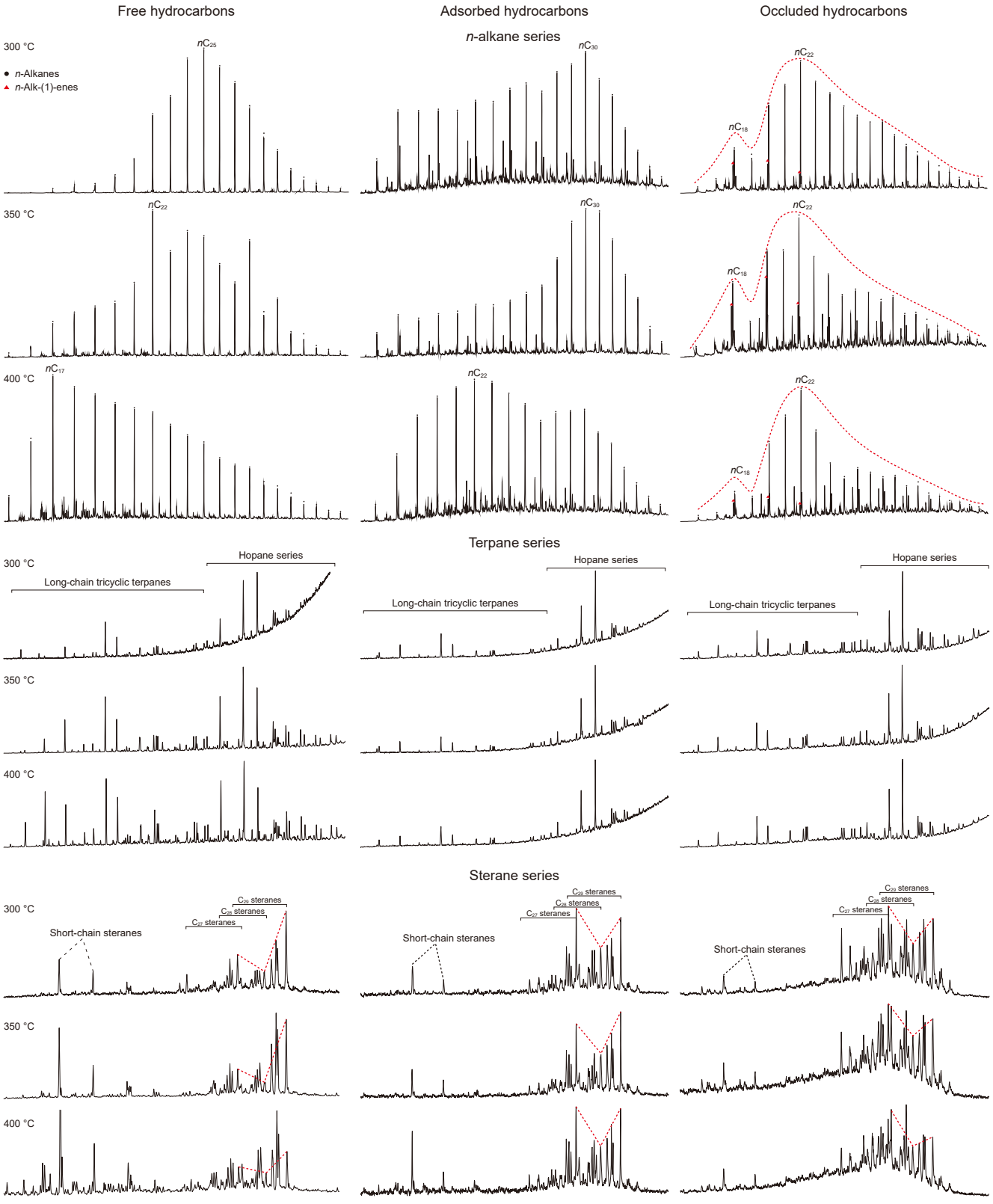

Fig. 5. Distributions of biomarkers in asphaltene thermal simulation products (The distributions of *n*-alkanes are based on on *m/z* 85 selected ion monitoring chromatograms; The distributions of terpanes are based on *m/z* 191 selected ion monitoring chromatograms; The distributions of steranes are based on *m/z* 217 selected ion monitoring chromatograms.) The drawing data comes from our previous study (Fang et al., 2022a).

Table 3
Selected biomarker parameters of the free and asphaltene-adsorbed/occluded fractions.

Parameter	State	Raw	300 °C	350 °C	400 °C	Range Min ~ Max	Δ (Max−Min)	$\delta^{13}C$ correlation
Tri/Pentacyclic terpane	Free	1.24	0.52	0.83	1.40	0.52~1.40	0.88	Strong
	Adsorbed	0.91	0.49	0.39	0.42	0.39~0.91	0.52	
	Occluded	0.69	0.54	0.57	0.54	0.54~0.69	0.15	
Ts/Tm	Free	0.45	0.27	0.05	0.06	0.05~0.45	0.40	Strong
	Adsorbed	1.08	0.65	0.61	0.54	0.54~1.08	0.54	
	Occluded	1.01	0.89	0.90	0.79	0.79~1.01	0.22	
$C_{29}Ts/C_{29}H$	Free	0.25	0.13	0.06	0.33	0.06~0.33	0.27	Strong
	Adsorbed	0.27	0.29	0.22	0.23	0.22~0.29	0.07	
	Occluded	0.32	0.37	0.37	0.33	0.32~0.37	0.05	
$C_{31}H$ 22S/(22S + 22R)	Free	0.57	0.55	0.53	0.52	0.52~0.57	0.05	Weak
	Adsorbed	0.54	0.56	0.54	0.55	0.54~0.56	0.02	
	Occluded	0.54	0.56	0.54	0.54	0.54~0.56	0.02	
$C_{21}P/C_{22}P$	Free	2.30	1.49	2.25	3.78	1.49~3.78	2.29	Strong
	Adsorbed	1.52	1.57	1.78	2.85	1.52~2.85	1.33	
	Occluded	1.37	1.39	1.58	1.72	1.37~1.72	0.35	
C_{21} ~ $C_{22}P/C_{27}$ ~ $C_{29}S$	Free	1.14	0.13	0.20	0.48	0.13~1.14	1.01	Strong
	Adsorbed	0.06	0.07	0.08	0.12	0.06~0.12	0.06	
	Occluded	0.08	0.05	0.08	0.06	0.05~0.08	0.03	
$C_{27}S/C_{27}$ ~ $C_{29}S$	Free	0.22	0.27	0.20	0.24	0.20~0.27	0.07	Weak
	Adsorbed	0.37	0.32	0.29	0.33	0.29~0.37	0.08	
	Occluded	0.32	0.36	0.31	0.34	0.31~0.36	0.05	
$C_{28}S/C_{27}$ ~ $C_{29}S$	Free	0.21	0.19	0.18	0.23	0.18~0.23	0.05	Weak
	Adsorbed	0.30	0.29	0.28	0.29	0.28~0.30	0.02	
	Occluded	0.34	0.26	0.28	0.30	0.26~0.34	0.08	
$C_{29}S/C_{27}$ ~ $C_{29}S$	Free	0.57	0.54	0.62	0.52	0.52~0.62	0.10	Weak
	Adsorbed	0.33	0.39	0.43	0.38	0.33~0.43	0.10	
	Occluded	0.34	0.38	0.41	0.36	0.34~0.41	0.07	
$C_{29}S\alpha\alpha\alpha$ 20S/(20S + 20R)	Free	0.54	0.34	0.46	0.58	0.34~0.58	0.24	Moderate
	Adsorbed	0.45	0.46	0.46	0.47	0.45~0.47	0.02	
	Occluded	0.48	0.46	0.47	0.49	0.46~0.49	0.03	
$C_{29}S\alpha\beta\beta/(\alpha\alpha\alpha+\alpha\beta\beta)$	Free	0.53	0.43	0.50	0.55	0.43~0.55	0.12	Moderate
	Adsorbed	0.38	0.40	0.42	0.41	0.38~0.42	0.04	
	Occluded	0.42	0.40	0.42	0.45	0.40~0.45	0.05	

Notes: "Raw" refers to the sample that have not been subjected to thermal simulation experiments. "$\delta^{13}C$ Correlation" refers to the degree of consistency with the change of $\delta^{13}C$ values (Table 1). The original biomarker data comes from our previous study (Fang et al., 2022a), where the specific meaning of parameter abbreviation can be found. Δ = Maximum value−minimum value across all samples (raw and thermal simulation temperatures of 300~400 °C), representing the total fluctuation range of parameters.

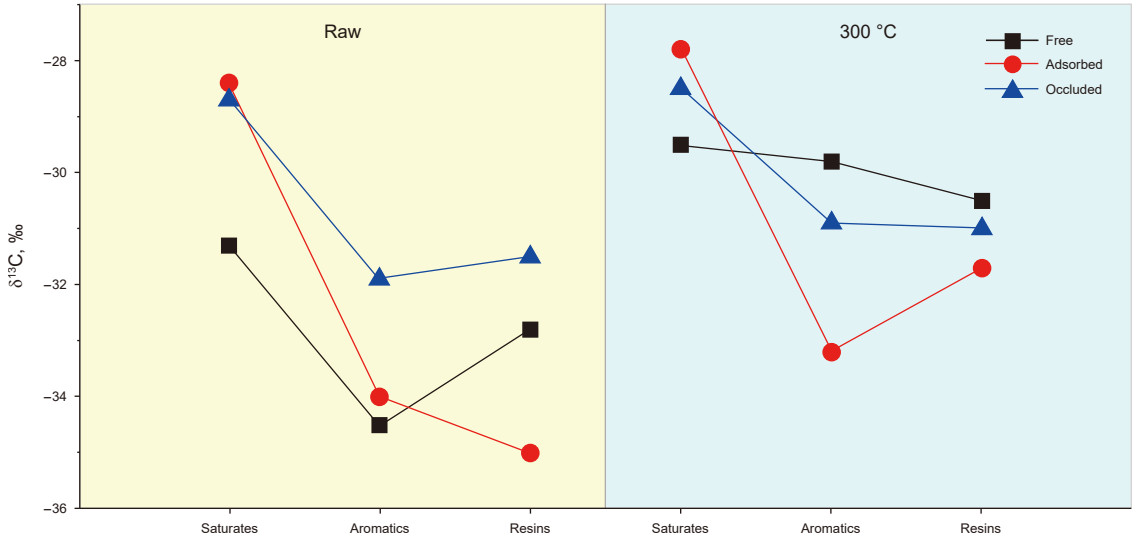

Fig. 6. Carbon isotopic compositions of free and asphaltene-adsorbed/occluded compound classes from DCM extracts of solid bitumen veins in the NW Sichuan Basin. "Raw" denotes the extracts from the original bitumen sample and "300 °C" refers to the extracts after gold tube pyrolysis of the isolated and purified asphaltenes at 300 °C for 24 h.

4.2. Maturation effect on $\delta^{13}C$ values of hydrocarbons in asphaltene structure

The $\delta^{13}C$ values of free/adsorbed saturated and aromatic hydrocarbons exhibited a decrease with increasing thermal stress, yet remained higher (enriched in ^{13}C) than the $\delta^{13}C$ values of parent asphaltenes (Fig. 7). A number of thermal simulation studies have demonstrated that during reactant cracking, the $\delta^{13}C$ value of hydrocarbon products undergoes a decrease followed by an increase (Galimov, 2006; Hill et al., 2003; Lorant et al., 1998; Tocqué et al., 2005). Actually, the evolution of $\delta^{13}C$ values with increasing thermal stress reflects a transition between two

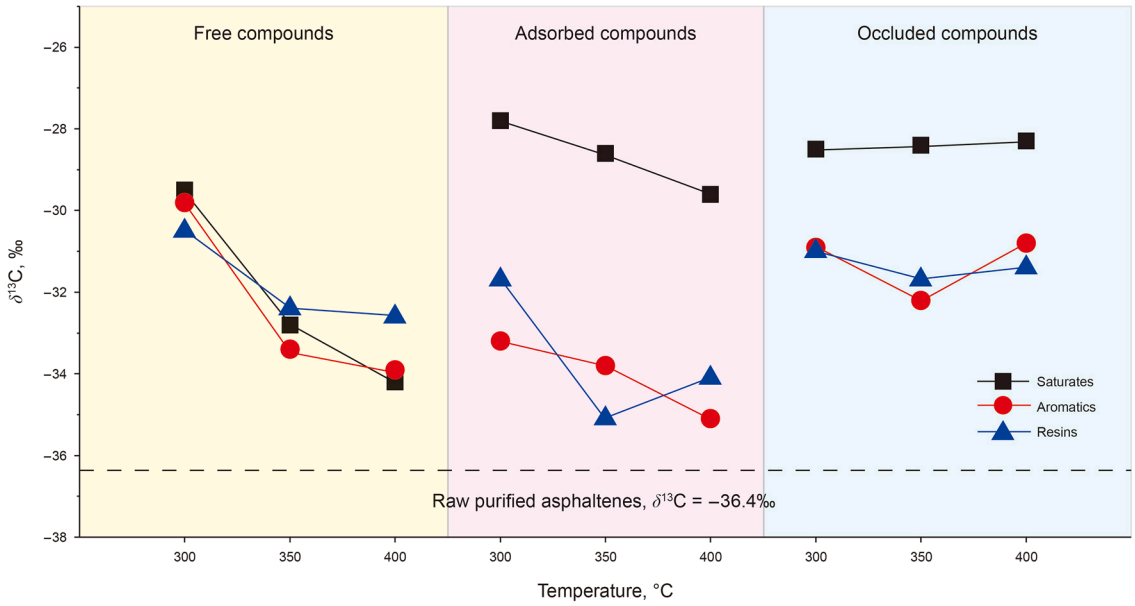

Fig. 7. Evolution of the carbon isotopic composition of compound classes during thermal maturation of purified asphaltenes in gold tubes for 24 h.

dominant mechanisms: the low-temperature release of pre-existing "residual carbon" and high-temperature cracking of the asphaltene matrix. At 300 °C, the observed enrichment in ^{13}C of the released hydrocarbons (the "residual carbon release effect") is interpreted primarily as a thermal desorption process (Galimov, 2006). This stage involves the mobilization and release of ^{13}C-enriched saturated hydrocarbons that were previously trapped within the asphaltene structure as a result of biodegradation, without significant thermal cracking of covalent bonds. As temperature increases to 350 °C and 400 °C, true thermal cracking becomes the dominant process. Here, the systematic decrease in $\delta^{13}C$ values for free and adsorbed hydrocarbons is driven by kinetic isotope effects (KIE) (Tocqué et al., 2005), wherein ^{12}C–^{12}C bonds within the asphaltene macromolecules are preferentially cleaved over ^{13}C-containing bonds due to their lower activation energy, leading to the generation of ^{12}C-enriched products. The potential inflection points in $\delta^{13}C$ at very high maturity, as suggested by the trend in adsorbed resins (Fig. 7), would mark the depletion of readily cleavable ^{12}C–^{12}C bonds, causing the residual pool to become progressively enriched in ^{13}C.

The yields of free maltenes increase with temperature, while the yields of asphaltene change inversely. Asphaltene-occluded saturated hydrocarbons exhibit significantly higher yields (0.7%–1.3%) compared to adsorbed saturated hydrocarbons (<0.3%) across all experimental temperatures (Table 2). This systematic trend supports the independence of occluded hydrocarbons. The consistently higher yields of occluded saturated hydrocarbons (even at 400 °C) reflect their protection within asphaltene nanoaggregates, which limits thermal cracking. In contrast, adsorbed saturated hydrocarbons (<0.3%) are more susceptible to degradation due to their exposed location on asphaltene surfaces. This aligns with prior studies showing that occluded biomarkers resist thermal alteration better than adsorbed/free counterparts (Cheng et al., 2017). In addition, the low yields of adsorbed saturated hydrocarbons confirm minimal contamination from residual free hydrocarbons during extraction. This underscores the reliability of dispersive solid-phase extraction (DSPE) protocol, which selectively isolates occluded components on the premise of excluding adsorbed components.

The carbon isotopic compositions of the occluded hydrocarbons derived from pyrolysis products were found to be similar to that of the original occluded components, with saturated hydrocarbons displaying a stable $\delta^{13}C$ value of around −28.5‰ (±0.2‰). Mild oxidation degradation has systematically confirmed that hydrocarbons occluded by macromolecules (kerogen or asphaltene) are shielded from secondary alterations (e.g., biodegradation) due to the protective effect of macromolecule structure (Cheng et al., 2017; Liao et al., 2006a; Yang et al., 2009). Thermal simulation experiments in semi-closed systems revealed that biomarker parameters (e.g., sterane/hopane parameters) of kerogen-occluded hydrocarbons remained stable across maturity stages (R_o = 0.49%–1.67%), unlike free hydrocarbons with obvious thermal evolution (Cheng et al., 2016). In addition, our prior gold-tube experiments showed that saturated and aromatic biomarkers in asphaltene-occluded hydrocarbons exhibited minimal compositional changes at 300–400 °C, supporting their thermal stability (Fang et al., 2022a, 2024). While $\delta^{13}C$ values of hydrocarbons in different occurrence states (free, asphaltene-adsorbed/occluded) were not explicitly reported in earlier studies, the variation law of distribution characteristics of biomarkers in different occurrence states is consistent with that of $\delta^{13}C$ values (Fig. 5), suggesting isotopic stability of occluded hydrocarbons.

The strong correlation between occluded biomarker stability and $\delta^{13}C$ invariance is mechanistically explained by the hierarchical protection effects of asphaltene. Ts/Tm and C_{31} 22S/(22S + 22R) ratios showed non-ideal maturity trends (Table 3), likely due to sedimentary-organic facies effects (Ts/Tm) and pre-existing equilibrium (C_{31} 22S/(22S + 22R) ratio), consistent with their known limitations in mature systems (Peters et al., 2004; Wang et al., 2000). The multistage aggregation structure of asphaltenes (Evdokimov and Fesan, 2016; Mullins, 2011) restricts thermal diffusion of occluded compounds (e.g., ΔTri/Pentacyclic terpane = 0.15; ΔC_{21}~$C_{22}P/C_{27}$~$C_{29}S$ = 0.03; Table 3), while free hydrocarbons undergo significant thermal cracking (e.g., ΔTri/Pentacyclic terpane = 0.88; ΔC_{21}~$C_{22}P/C_{27}$~$C_{29}S$ = 1.01; Table 3). This aligns with our observation that *n*-(1)-alkenes persist in occluded fractions even at 400 °C (Fig. 5), whereas free *n*-alkanes show progressive carbon-number shifts (Fig. 5). The stability of

biomarkers thus mirrors $\delta^{13}C$ invariance because occluded compounds are shielded within asphaltene nanoaggregates (~2 nm), where limited exposure to thermal/chemical reactions preserves primary molecular and isotopic signatures. Critically, adsorbed biomarkers (molecular composition and biomarker parameters) exhibit transitional properties between free and occluded fractions (Table 3; Fig. 5), reflecting their partial shielding by asphaltene peripheries. The intermediate behavior of adsorbed hydrocarbons arises from their partial protection by asphaltene peripheries: Adsorbed components reside on asphaltene surfaces, making them more susceptible to thermal/chemical alterations than occluded (core-shielded) but less than free (unbound) hydrocarbons; Adsorbed components may exchange with free fractions during thermal stress, explaining their transitional isotopic/molecular signatures. This supports a hierarchical protection model: free > adsorbed > occluded in susceptibility to alteration. For source correlation, only occluded fractions meet dual criteria: thermal stability and carbon isotopic consistency. These findings validate asphaltene-occluded biomarkers as robust proxies for oil-source studies, particularly in reservoirs with secondary alterations.

4.3. Indication for the source of solid bitumen from the Kuangshanliang area

The $\delta^{13}C$ values of asphaltene-occluded saturated hydrocarbons (approximately −28.5‰) are evidently higher (enriched in ^{13}C) than the $\delta^{13}C$ values (−38.4‰ ~ −34.0‰) of Lower Cambrian bitumens or oil seeps from the same area (Fang et al., 2022c; Huang and Wang, 2008; Wang et al., 2014; Wu et al., 2012). The free fractions in bitumen obtained by conventional fractionation methods are characteristically ^{13}C-poor, which is often attributed to the preferential consumption by cyanobacteria of ^{12}C in CO_2 through photosynthesis, producing organic matter with lower (enriched in ^{12}C) carbon isotope values (Huang and Wang, 2008). However, secondary alterations, such as biodegradation, can entirely alter the carbon isotope composition of sedimentary organic matter. Consequently, the biogenic sources and sedimentary environments of organic matter cannot be directly inferred from the isotopic compositions of the bitumen sample that have undergone moderate-to-severe biodegradation (Fang et al., 2021, 2022c; Wang et al., 2014).

In contrast, the carbon isotope values of asphaltene-occluded hydrocarbons can more reliably reveal the original organic matter source of the bitumen. It is noteworthy that $\delta^{13}C_{org}$ values of source rock alone may not reliably distinguish between the Doushantuo IV Member (−33.4‰ to −34.9‰) and the Lower Cambrian Qiongzhusi Formation (−29.2‰ to −34.9‰) in the study area (Fang et al., 2022c). This overlap contrasts with the facies-dependent $\delta^{13}C_{org}$ trends reported by Fang et al. (2019), where shallow-water platform deposits of the Doushantuo Formation source rock (Members II and IV; −26‰ to −31‰) exhibited systematically heavier values than the Qiongzhusi Formation source rock (−30‰ to −35‰) in the same spatial positions. The anomalously light $\delta^{13}C_{org}$ values observed in our Doushantuo IV Member samples likely reflect deposition in the lower slope-basin transition zone, where isotopic values span a wider range (−25‰ to −39‰). Paleogeographic reconstructions (Liu et al., 2018) confirm the northern Sichuan Basin's adjacency to the paleo-Tethyan Ocean during the Ediacaran-Cambrian transition, explaining the observed facies-dependent $\delta^{13}C_{org}$ variations (Jiang et al., 2010; Wang et al., 2016b) that preclude extrapolating these anomalies to the region's dominant shallow-water platform facies. Therefore, significant differences in organic carbon isotopes between the Ediacaran Doushantuo Formation and the Cambrian Qiongzhusi Formation source rocks in the shallow water facies area (platform and upper slope) are used to distinguish two sets of source rocks, with isotopic compositions ranging from −26‰ to −31‰ and from −30‰ to −35‰, respectively (Fang et al., 2019, 2022c). Critically, the $\delta^{13}C$ values of the asphaltene-occluded saturated hydrocarbons in this study agree well with those of the Ediacaran Doushantuo Formation source rock (Fig. 8), supporting the view that the bitumen veins originate from the source rocks of the Doushantuo Formation (Han et al., 2022).

Notably, the carbon isotope values of soluble organic matter and free saturated hydrocarbons in solid bitumen were significantly lower (enriched in ^{12}C) than those of asphaltene-occluded saturated hydrocarbons. The former was consistent with the $\delta^{13}C$ values reported previously for solid bitumens and oil seeps in the area (Fig. 8). This suggests that secondary alteration has affected the carbon isotope values of bitumens or oil seeps on exposed ground, making them unsuitable for source rock-oil correlation.

On the other hand, unlike free and adsorbed biomarkers that are prone to alterations, the occluded biomarkers also provide a reliable indication of the source of organic matter, which has not been clearly revealed in previous reports (Fang et al., 2022a). The distribution characteristics of occluded *n*-alkanes exhibited a "bimodal state", and the relative abundance of the subsequent peak (main peak nC_{22}) was greater than that of the previous peak (main peak nC_{18}) (Fig. 4). This "bimodal" trait may be independent of maturity and may represent contributions from two types of algae (Liang et al., 2009). In addition, the input of bacteria and fungi can also produce C_{14}~C_{22} *n*-alkanes, and it often shows a strong advantage of individual carbon numbers (Grimalt et al., 1986; Nishimura and Baker, 1986), which is consistent with the advantages of nC_{18} and nC_{22} described above. Furthermore, hopane series compounds in occluded hydrocarbons are also common signs of bacterial input (Wang et al., 2020). Therefore, both algae and microorganisms may be parent sources of organic matter. It should be noted that the microbial contribution here is mainly reflected in its direct input in the formation of sedimentary organic matter, which is not the same as the secondary alteration of organic matter in the middle and late diagenesis by biodegradation. The original information of the former may be retained in asphaltene-occluded hydrocarbons, so that the role of the latter will not change this information again.

Compared with the free steranes (dominated by C_{29} steranes) (Huang and Wang, 2008; Wang et al., 2014), the relative

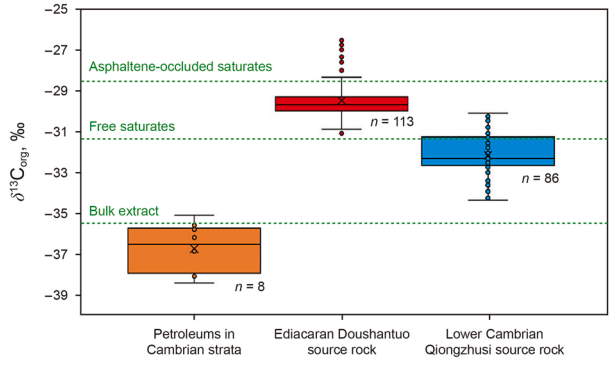

Fig. 8. The bulk $\delta^{13}C_{org}$ values for the Ediacaran and Cambrian petroleum systems (including source rocks, oil seeps and bitumen veins) and the potential source rocks in the northwest Sichuan Basin. The different types of hydrocarbons and the source rocks are marked in different colors (The data source is quoted from Fang et al. (2019)). Petroleums in Cambrian strata denote oil seeps and bitumen veins from Cambrian strata. The Doushantuo source rocks are from shallow platform facies. The Qiongzhusi source rock contains its time equivalents strata (Niutitang Formation). The letter "*n*" represents the number of samples.

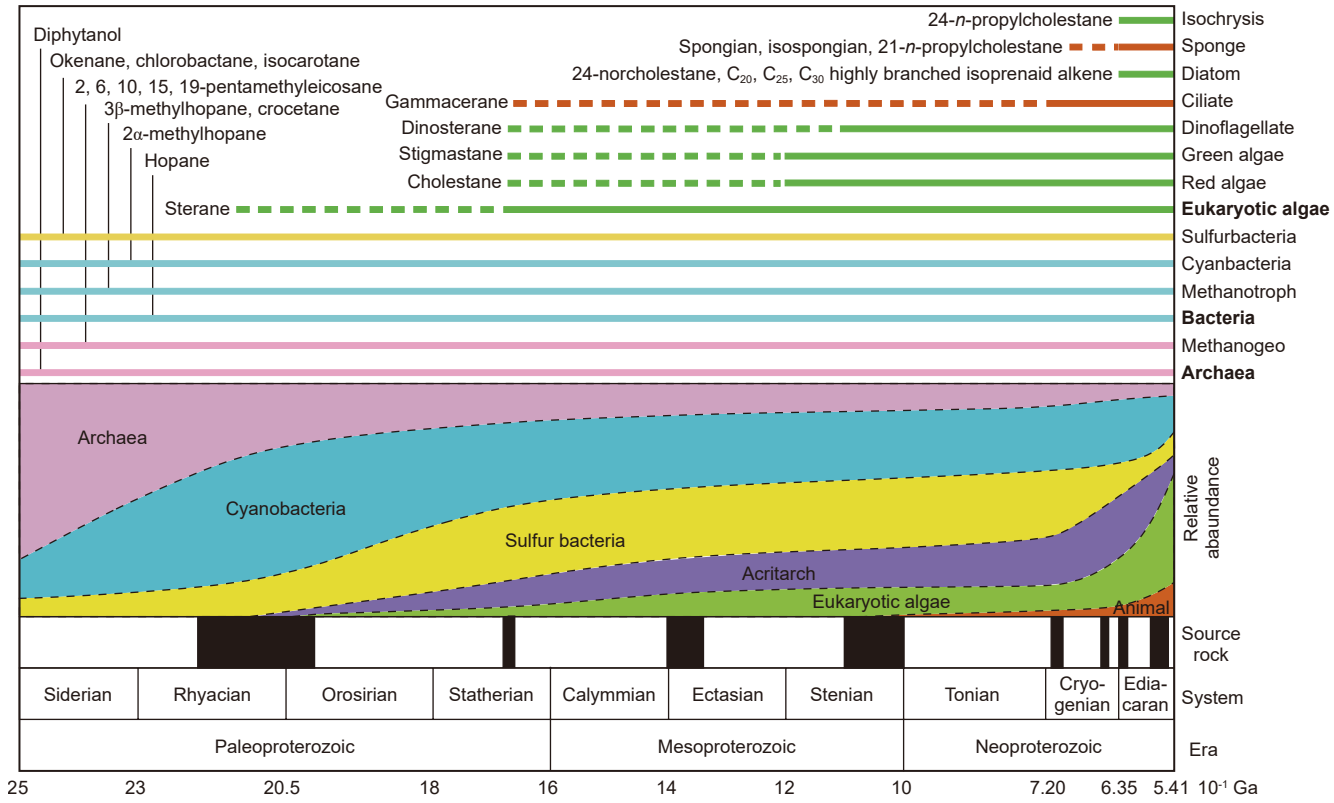

Fig. 9. Proterozoic biological evolution trends and their biomarker evidence (Zhao et al., 2019).

abundance of C_{27} steranes in occluded steranes is obviously higher (Fig. 4). The dominance of C_{29} steranes in free hydrocarbons from the bitumen has been postulated to reflect the contribution of cyanobacteria or green algae during the Early Paleozoic and preceding periods (Ge et al., 2018; Grantham, 1986; Volkman, 1986; Wang et al., 2014). However, a recent study has demonstrated that the dominance of C_{29} steranes in free hydrocarbons from the bitumen is the result of biodegradation (Fang et al., 2021). Therefore, the distribution of steranes in occluded hydrocarbons may be a more reliable indicator of the source of sedimentary organic matter.

The C_{27} sterane dominance can be traced back to the evolution of life in the Precambrian period. The evolution of eukaryotes from prokaryotes occurred during the Proterozoic period (Fig. 8). However, it was not until an interval between global glaciations known as Snowball Earth, which occurred during the Neoproterozoic Oxygenation Event (NOE), that eukaryotic algae radiated to become the major oxygen producers (Brocks et al., 2017). C_{27} steranes are the dominant compounds in rock extracts from the Kwagunt Formation (~0.74 Ga) of the Chuar Group and the Red Pine Shale (~0.74 Ga) of the Uinta Mountain Group in North America, indicating that eukaryotic algae had become the primary source of sedimentary organic matter at that time (Summons et al., 1988; Vogel et al., 2005). The appearance of fossils of complex macroscopic algae, benthic algae, and metazoans during the Doushantuo interval in the Yangtze region, southern China, marks a significant milestone in the evolution of life on Earth (Chen et al., 2014; Yuan et al., 2011). Furthermore, the Neoproterozoic black shales in which C_{27} sterane is dominant have also been identified in the Yangtze region, providing evidence that eukaryotic algae contributed to the formation of Precambrian sedimentary organic matter (Wang et al., 2008).

Although due to the high maturity and the limitations of the samples, the biomarkers in the source rocks of the Doushantuo Formation have not been recognized as consistent distribution characteristics. The distribution of steranes in occluded hydrocarbons suggests that the primary biogenic source of bitumen is likely to be eukaryotic algae, which is consistent with the biological source of high-quality source rocks in Doushantuo Formation (Zhu et al., 2021). From the perspective of biological evolution, the expansion of eukaryotic algae in the Neoproterozoic (Wang et al., 2019) suggests a greater capacity for the production of organic matter compared to prokaryotic bacteria (Fig. 9). Consequently, eukaryotic algae provide a material basis for the widespread distribution of Neoproterozoic source rocks and are an important source of Precambrian sedimentary organic matter including paleo-oil reservoirs of the Dengying Formation and derived surface bitumens. These evidences support the consistency of $\delta^{13}C$ values of asphaltene-occluded hydrocarbons with those of source rocks of Doushantuo Formation.

5. Conclusions

(1) The $\delta^{13}C$ values of the saturated hydrocarbons of the free maltenes extracted from solid (vein) bitumen of NW Sichuan are significantly higher (enriched in ^{13}C) than those of the aromatic and polar components. All asphaltene-associated "occluded" compound groups have higher $\delta^{13}C$ values (are enriched in ^{13}C) than the free ones. This holds especially for the saturated hydrocarbons.

(2) Thermal maturation experiments demonstrate that the $\delta^{13}C$ values of the free and asphaltene-adsorbed components decrease with temperature. At low thermal stress, the release of isotopically heavy "residual carbon" compounds

from the asphaltene matrix is the dominant process. With increasing thermal stress, asphaltenes decompose, resulting in the preferential scission of ^{12}C–^{12}C bonds and release of isotopically lighter compounds. This process ultimately explains the decrease in the $\delta^{13}C$ values of free and adsorbed hydrocarbons with thermal evolution.

(3) The $\delta^{13}C$ value of asphaltene-occluded components remains unaltered throughout the thermal maturation experiment, thereby reflecting the isotopic composition of the original organic matter. This evidence confirms that the asphaltene structure effectively protects and isolates the occluded components. The $\delta^{13}C$ values of asphaltene-occluded components remain constant regardless of maturity ($R_o < 1.5\%$) and are in agreement with the $\delta^{13}C_{org}$ (the bulk organic carbon isotope) value of the source rock of the Doushantuo Formation. Future studies should include bitumen samples from different locations to further verify the robustness of asphaltene-occluded hydrocarbons as a universal tool for oil-source correlation in altered systems.

CRediT authorship contribution statement

Peng Fang: Writing – original draft, Methodology, Investigation, Funding acquisition, Formal analysis. **Jia Wu:** Writing – review & editing, Supervision, Methodology, Funding acquisition. **Xue-Min Xu:** Writing – review & editing, Supervision, Methodology. **Bin Shen:** Writing – review & editing, Supervision. **Wei-Lin Sun:** Writing – review & editing. **Xiao Jin:** Validation, Data curation. **Feng Chen:** Writing – review & editing, Data curation. **Ning-Ning Zhong:** Writing – review & editing, Resources, Conceptualization. **Ming-Hui Zhou:** Writing – review & editing.

Declaration of interests

The authors declare that they have no known competing financial interests or personal relationships that could have appeared to influence the work reported in this paper.

Acknowledgement

We would like to express our gratitude to Shuo Gao and Tiantian Li for their help with the experiments. This work was granted by National Natural Science Foundation of China (No. 42503040), the Chinese Academy of Geological Sciences Basal Research Fund (No. CSJ-2024-05) and the State Key Laboratory of Organic Geochemistry, GIGCAS (No. SKLOG202123).

Supplementary materials

Supplementary materials to this article can be found online at https://doi.org/10.1016/j.petsci.2025.11.024.

References

Brocks, J.J., Jarrett, A.J.M., Sirantoine, E., et al., 2017. The rise of algae in Cryogenian oceans and the emergence of animals. Nature 548 (7669), 578–581. https://doi.org/10.1038/nature23457.

Bushnev, D.A., Burdel'Naya, N.S., 2009. Kerogen: chemical structure and formation conditions. Russ. Geol. Geophys. 50 (7), 638–643. https://doi.org/10.1016/j.rgg.2008.12.004.

Chen, L., Xiao, S., Pang, K., et al., 2014. Cell differentiation and germ–soma separation in Ediacaran animal embryo-like fossils. Nature 516 (7530), 238–241. https://doi.org/10.1038/nature13766.

Cheng, B., Du, J., Tian, Y., et al., 2016. Thermal evolution of adsorbed/occluded hydrocarbons inside kerogens and its significance as exemplified by one low-matured kerogen from Santanghu Basin, Northwest China. Energy Fuel. 30 (6), 4529–4536. https://doi.org/10.1021/acs.energyfuels.6b00218.

Cheng, B., Zhao, J., Yang, C., et al., 2017. Geochemical evolution of occluded hydrocarbons inside geomacromolecules: A review. Energy Fuel. 31 (9), 8823–8832. https://doi.org/10.1021/acs.energyfuels.7b00454.

Chung, H.M., Brand, S.W., Grizzle, P.L., 1981. Carbon isotope geochemistry of Paleozoic oils from big horn Basin. Geochem. Cosmochim. Acta 45 (10), 1803–1815. https://doi.org/10.1016/0016-7037(81)90011-9.

Evdokimov, I.N., Fesan, A.A., 2016. Multi-step formation of asphaltene colloids in dilute solutions. Coll. Surf. A Physicochem. Eng. Aspect. 492, 170–180. https://doi.org/10.1016/j.colsurfa.2015.11.072.

Fang, P., Hong, Z., Wu, J., et al., 2024. The influence of asphaltene matrix on the thermal evolution of polycyclic aromatic hydrocarbons: Experimental evidence and geochemical implications. J. Asian Earth Sci. 259, 105927. https://doi.org/10.1016/j.jseaes.2023.105927.

Fang, P., Wu, J., Chen, F., et al., 2022a. The hysteresis of asphaltene-trapped saturated hydrocarbons during thermal evolution. Fuel 329, 125374. https://doi.org/10.1016/j.fuel.2022.125374.

Fang, P., Wu, J., Li, B., et al., 2022b. Nondestructive investigation on hydrocarbons occluded in asphaltene matrix: The evidence from the dispersive solid-phase extraction. J. Petrol. Sci. Eng. 217, 110890. https://doi.org/10.1016/j.petrol.2022.110890.

Fang, P., Wu, J., Li, B., et al., 2021. Comparison of separation of asphaltene adsorbed hydrocarbons by different elution methods. Acta Pet. Sin. 42 (5), 623–633. https://doi.org/10.7623/syxb202105006 (in Chinese).

Fang, X., Geng, A., Liang, X., et al., 2022c. Comparison of the Ediacaran and Cambrian petroleum systems in the Tianjingshan and the Micangshan uplifts, northern Sichuan Basin, China. Mar. Petrol. Geol., 105876 https://doi.org/10.1016/j.marpetgeo.2022.105876.

Fang, X., Wu, L., Geng, A., et al., 2019. Formation and evolution of the Ediacaran to Lower Cambrian black shales in the Yangtze Platform, South China. Palaeogeogr. Palaeoclimatol. Palaeoecol. 527, 87–102. https://doi.org/10.1016/j.palaeo.2019.04.025.

Galimov, E.M., 2006. Isotope organic geochemistry. Org. Geochem. 37 (10), 1200–1262. https://doi.org/10.1016/j.orggeochem.2006.04.009.

Ge, X., Shen, C., Selby, D., et al., 2018. Petroleum-generation timing and source in the northern Longmen Shan thrust belt, Southwest China: Implications for multiple oil-generation episodes and sources. AAPG Bull. 102 (5), 913–938. https://doi.org/10.1306/0711171623017125.

Grantham, P.J., 1986. The occurrence of unusual C_{27} and C_{29} sterane predominances in two types of Oman crude oil. Org. Geochem. 9 (1), 1–10. https://doi.org/10.1016/0146-6380(86)90077-X.

Grimalt, J., Albaigés, J., Alexander, G., et al., 1986. Predominance of even carbon-numbered n-alkanes in coal seam samples of Nograd Basin (Hungary). Naturwissenschaften 73 (12), 729–731. https://doi.org/10.1007/BF00399242.

Han, K., Wang, G., Wang, T., et al., 2022. Occurrence and genetic mechanism of large asphaltic veins at the Longmenshan Fronthill Belt, Western Yangtze Craton, South China. In: Han, K., Wang, G., Wang, T., Wang, L. (Eds.), Meso-Neoproterozoic Geology and Petroleum Resources in China. Springer Nature Singapore, Singapore, pp. 539–563. https://doi.org/10.1007/978-981-19-5666-9_15.

Hill, R.J., Tang, Y., Kaplan, I.R., 2003. Insights into oil cracking based on laboratory experiments. Org. Geochem. 34 (12), 1651–1672. https://doi.org/10.1016/S0146-6380(03)00173-6.

Huang, D.F., Wang, L.S., 2008. Geochemical characteristics of bituminous dike in Kuangshanliang area of the Northwestern Sichuan Basin and its significance. Acta Pet. Sin. 29 (1), 23–28 (in Chinese).

Jia, W., Chen, S., Zhu, X., et al., 2017. D/H ratio analysis of pyrolysis-released *n*-alkanes from asphaltenes for correlating oils from different sources. J. Anal. Appl. Pyrolysis 126, 99–104. https://doi.org/10.1016/j.jaap.2017.06.020.

Jiang, G., Wang, X., Shi, X., et al., 2010. Organic carbon isotope constraints on the dissolved organic carbon (DOC) reservoir at the Cryogenian–Ediacaran transition. Earth Planet Sci. Lett. 299 (1–2), 159–168. https://doi.org/10.1016/j.epsl.2010.08.031.

Kashirtsev, V.A., 2018. Hydrocarbons occluded by asphaltenes. Russ. Geol. Geophys. 59 (8), 975–982. https://doi.org/10.1016/j.rgg.2018.07.017.

Landais, P., Michels, R., Poty, B., et al., 1989. Pyrolysis of organic matter in cold-seal pressure autoclaves. Experimental approach and applications. J. Anal. Appl. Pyrolysis 16 (2), 103–115. https://doi.org/10.1016/0165-2370(89)85010-7.

Lewan, M.D., 1983. Effects of thermal maturation on stable organic carbon isotopes as determined by hydrous pyrolysis of Woodford Shale. Geochem. Cosmochim. Acta 47 (8), 1471–1479. https://doi.org/10.1016/0016-7037(83)90306-X.

Li, K., Zhao, Z., Lu, H., et al., 2022. Effects of inherent pyrite on hydrocarbon generation by thermal pyrolysis: an example of low maturity type-II kerogen from Alum shale formation, Sweden. Fuel 312, 122865. https://doi.org/10.1016/j.fuel.2021.122865.

Liang, D., Tonglou, G., Chen, J., 2009. Geochemical characteristics of four suits of regional marine source rocks, South China. Mar. Orig. Petrol. Geol. 14, 1–15 (in Chinese).

Liang, T., Zhan, Z.W., Gao, Y., et al., 2020. Molecular structure and origin of solid bitumen from northern Sichuan Basin. Mar. Petrol. Geol. 122, 104654. https://doi.org/10.1016/j.marpetgeo.2020.104654.

Liao, Z., Geng, A., Graciaa, A., et al., 2006a. Different adsorption/occlusion properties of asphaltenes associated with their secondary evolution processes in oil reservoirs. Energy Fuel. 20 (3), 1131–1136. https://doi.org/10.1021/ef050355+.

Liao, Z., Geng, A., Graciaa, A., et al., 2006b. Saturated hydrocarbons occluded inside asphaltene structures and their geochemical significance, as exemplified by

two Venezuelan oils. Org. Geochem. 37 (3), 291–303. https://doi.org/10.1016/j.orggeochem.2005.10.010.
Liao, Z., Graciaa, A., Geng, A., et al., 2006c. A new low-interference characterization method for hydrocarbons occluded inside asphaltene structures. Appl. Geochem. 21 (5), 833–838. https://doi.org/10.1016/j.apgeochem.2006.02.005.
Liu, S., Deng, B., Sun, W., et al., 2018. Sichuan Basin: A superimposed sedimentary basin mainly controlled by its peripheric tectonics. Chin. J. Geol. 53 (1), 308–326. https://doi.org/10.12017/dzkx.2018.018 (in Chinese).
Lorant, F., Behar, F., 2002. Late generation of methane from mature kerogens. Energy Fuel. 16 (2), 412–427. https://doi.org/10.1021/ef010126x.
Lorant, F., Prinzhofer, A., Behar, F., et al., 1998. Carbon isotopic and molecular constraints on the formation and the expulsion of thermogenic hydrocarbon gases. Chem. Geol. 147 (3), 249–264. https://doi.org/10.1016/S0009-2541(98)00017-5.
Ma, A., Zhang, S., Zhang, D., 2008. Ruthenium-ion-catalyzed oxidation of asphaltenes of heavy oils in Lunnan and Tahe oilfields in Tarim Basin, NW China. Org. Geochem. 39 (11), 1502–1511. https://doi.org/10.1016/j.orggeochem.2008.07.016.
Meredith, W., Snape, C.E., Carr, A.D., et al., 2008. The occurrence of unusual hopenes in hydropyrolysates generated from severely biodegraded oil seep asphaltenes. Org. Geochem. 39 (8), 1243–1248. https://doi.org/10.1016/j.orggeochem.2008.01.022.
Michels, R., Landais, P., 1994. Artificial coalification: Comparison of confined pyrolysis and hydrous pyrolysis. Fuel 73 (11), 1691–1696. https://doi.org/10.1016/0016-2361(94)90154-6.
Monthioux, M., Landais, P., Monin, J.-C., 1985. Comparison between natural and artificial maturation series of humic coals from the Mahakam delta, Indonesia. Org. Geochem. 8 (4), 275–292. https://doi.org/10.1016/0146-6380(85)90006-3.
Mullins, O.C., 2011. The asphaltenes. Annu. Rev. Anal. Chem. 4, 393–418. https://doi.org/10.1146/annurev-anchem-061010-113849.
Nishimura, M., Baker, E.W., 1986. Possible origin of n-alkanes with a remarkable even-to-odd predominance in recent marine sediments. Geochem. Cosmochim. Acta 50 (2), 299–305. https://doi.org/10.1016/0016-7037(86)90178-X.
Orea, M., López, L., Ranaudo, M.A., et al., 2021. Saturated biomarkers adsorbed and occluded by the asphaltenes of some Venezuelan crude oils: Limitations in geochemical assessment and interpretations. J. Petrol. Sci. Eng. 206, 109048. https://doi.org/10.1016/j.petrol.2021.109048.
Pan, C., Geng, A., Liao, Z., et al., 2002. Geochemical characterization of free versus asphaltene-sorbed hydrocarbons in crude oils: Implications for migration-related compositional fractionations. Mar. Petrol. Geol. 19 (5), 619–632. https://doi.org/10.1016/S0264-8172(02)00031-4.
Peters, K.E., Walters, C.C., Moldowan, J.M., 2004. The biomarker guide: Volume 2: Biomarkers and isotopes in petroleum systems and earth history, vol. 2. Cambridge University Press, Cambridge.
Snowdon, L.R., Volkman, J.K., Zhang, Z., et al., 2016. The organic geochemistry of asphaltenes and occluded biomarkers. Org. Geochem. 91, 3–15. https://doi.org/10.1016/j.orggeochem.2015.11.005.
Stahl, W.J., 1977. Carbon and nitrogen isotopes in hydrocarbon research and exploration. Chem. Geol. 20 (2), 121–149. https://doi.org/10.1016/0009-2541(77)90041-9.
Stahl, W.J., 1978. Source rock-crude oil correlation by isotopic type-curves. Geochem. Cosmochim. Acta 42 (10), 1573–1577. https://doi.org/10.1016/0016-7037(78)90027-3.
Stahl, W.J., 1980. Compositional changes and $^{13}C/^{12}C$ fractionations during the degradation of hydrocarbons by bacteria. Geochem. Cosmochim. Acta 44 (11), 1903–1907. https://doi.org/10.1016/0016-7037(80)90238-0.
Summons, R.E., Brassell, S.C., Eglinton, G., et al., 1988. Distinctive hydrocarbon biomarkers from fossiliferous sediment of the late proterozoic Walcott member, Chuar Group, Grand Canyon, Arizona. Geochem. Cosmochim. Acta 52 (11), 2625–2637. https://doi.org/10.1016/0016-7037(88)90031-2.
Sweeney, J., Burnham, A., 1990. Evaluation of a simple model of vitrinite reflectance based on chemical kinetics. AAPG Bull. 74 (10), 1559–1570. https://doi.org/10.1306/0C9B251F-1710-11D7-8645000102C1865D.
Tian, Y., Yang, C., Liao, Z., et al., 2012a. Geochemical quantification of mixed marine oils from Tazhong area of Tarim Basin, NW China. J. Petrol. Sci. Eng. 90–91, 96–106. https://doi.org/10.1016/j.petrol.2012.04.028.
Tian, Y., Zhao, J., Yang, C., et al., 2012b. Multiple-sourced features of marine oils in the Tarim Basin, NW China – geochemical evidence from occluded hydrocarbons inside asphaltenes. J. Asian Earth Sci. 54–55, 174–181. https://doi.org/10.1016/j.jseaes.2012.04.010.
Tocqué, E., Behar, F., Budzinski, H., et al., 2005. Carbon isotopic balance of kerogen pyrolysis effluents in a closed system. Org. Geochem. 36 (6), 893–905. https://doi.org/10.1016/j.orggeochem.2005.01.007.
Vogel, M.B., Moldowan, J.M., Zinniker, D., 2005. Biomarkers from units in the Uinta Mountain and Chuar groups. AAPG/Datapages Comb. Publ. Datab. 75–96.
Volkman, J.K., 1986. A review of sterol markers for marine and terrigenous organic matter. Org. Geochem. 9 (2), 83–99. https://doi.org/10.1016/0146-6380(86)90089-6.
Wang, C., Fu, J., Sheng, G., et al., 2000. Geochemical characteristics and applications of 18α (H)-neohopanes and 17α (H)-diahopanes. Chin. Sci. Bull. 45 (19), 1742–1748. https://doi.org/10.1360/csb2000-45-13-1366.
Wang, G., Han, K., Wang, L., et al., 2014. Organic geochemical characteristics and origin of solid bitumen and oil sands in northwestern Sichuan. Petrol. Geol. Exp. 36 (6), 731–735. https://doi.org/10.11781/sysydz201406731 (in Chinese).
Wang, H., Zhang, S., Wang, X., et al., 2020. Hydrocarbon generation from bacterial biomass in ca. 1320 million years ago. IOP Conf. Ser. Earth Environ. Sci. 600 (1), 012032. https://doi.org/10.1088/1755-1315/600/1/012032.
Wang, J., Tenger, Liu, W., et al., 2016a. Definition of petroleum generating time for Lower Cambrian bitumen of the Kuangshanliangin the west Sichuan Basin, China: Evidence from Re-Os isotopic isochron age. Nat. Gas Geosci. 27, 1290–1298. https://doi.org/10.11764/j.issn.1672-1926.2016.07.1290 (in Chinese).
Wang, N., Li, M., Hong, H., et al., 2019. Biological sources of sedimentary organic matter in Neoproterozoic–Lower Cambrian shales in the Sichuan Basin (SW China): Evidence from biomarkers and microfossils. Palaeogeogr. Palaeoclimatol. Palaeoecol. 516, 342–353. https://doi.org/10.1016/j.palaeo.2018.12.012.
Wang, T., Han, K., 2011. On Meso-Neoproterozoic primary petroleum resources. Acta Pet. Sin. 32 (1), 1–7 (in Chinese).
Wang, T.G., Li, M., Wang, C., et al., 2008. Organic molecular evidence in the Late Neoproterozoic Tillites for a palaeo-oceanic environment during the snowball Earth era in the Yangtze region, southern China. Precambr. Res. 162 (3–4), 317–326. https://doi.org/10.1016/j.precamres.2007.09.009.
Wang, X., Jiang, G., Shi, X., et al., 2016b. Paired carbonate and organic carbon isotope variations of the Ediacaran Doushantuo Formation from an upper slope section at Siduping, South China. Precambr. Res. 273, 53–66. https://doi.org/10.1016/j.precamres.2015.12.010.
Wu, J., Fang, P., Wang, X.C., et al., 2020. The potential occurrence modes of hydrocarbons in asphaltene matrix and its geochemical implications. Fuel 278, 118233. https://doi.org/10.1016/j.fuel.2020.118233.
Wu, J., Ji, F., Wang, Y., et al., 2022. Influence of hydrogen fugacity on thermal transformation of sedimentary organic matter: implications for hydrocarbon generation in the ultra-depth. Sci. China Earth Sci. 65, 2188–2201. https://doi.org/10.1007/s11430-022-9957-y.
Wu, J., Qi, W., Jiang, F.J., et al., 2021. Influence of sulfate on the generation of bitumen components from kerogen decomposition during catagenesis. Pet. Sci. 18 (6), 1611–1618. https://doi.org/10.1016/j.petsci.2021.09.029.
Wu, L., Liao, Y., Fang, Y., et al., 2012. The study on the source of the oil seeps and bitumens in the Tianjingshan structure of the northern Longmen Mountain structure of Sichuan Basin, China. Mar. Petrol. Geol. 37 (1), 147–161. https://doi.org/10.1016/j.marpetgeo.2012.05.011.
Xiong, Y., Geng, A., 2000. Carbon isotopic composition of individual *n*-alkanes in asphaltene pyrolysates of biodegraded crude oils from the Liaohe Basin, China. Org. Geochem. 31 (12), 1441–1449. https://doi.org/10.1016/S0146-6380(00)00083-8.
Yang, C., Liao, Z., Zhang, L., et al., 2009. Some biogenic-related compounds occluded inside asphaltene aggregates. Energy Fuel. 23 (1), 820–827. https://doi.org/10.1021/ef8007294.
Yuan, X., Chen, Z., Xiao, S., et al., 2011. An early Ediacaran assemblage of macroscopic and morphologically differentiated eukaryotes. Nature 470 (7334), 390–393. https://doi.org/10.1038/nature09810.
Zhao, J., Liao, Z., Zhang, L., et al., 2010. Comparative studies on compounds occluded inside asphaltenes hierarchically released by increasing amounts of H_2O_2/CH_3COOH. Appl. Geochem. 25 (9), 1330–1338. https://doi.org/10.1016/j.apgeochem.2010.06.003.
Zhao, W., Wang, X., Hu, S., et al., 2019. Hydrocarbon generation characteristics and exploration prospects of Proterozoic source rocks in China. Sci. China Earth Sci. 62 (6), 909–934. https://doi.org/10.1007/s11430-018-9312-4.
Zhu, G., Zhao, K., Li, T., et al., 2021. Formation mechanism and distribution prediction of source rocks in the Ediacaran Doushantuo Formation, South China. Acta Geol. Sin. 95 (8), 2553–2574. https://doi.org/10.19762/j.cnki.dizhixuebao.2020277 (in Chinese).
Zhu, Z., Li, M., Li, J., et al., 2022. Identification, distribution and geochemical significance of dinaphthofurans in coals. Org. Geochem., 104399 https://doi.org/10.1016/j.orggeochem.2022.104399.